

# Collisions with Black Holes and Deconfined Plasmas

---

**Aaron J. Amsel, Donald Marolf, and Amitabh Virmani**

*Department of Physics, University of California at Santa Barbara, Santa Barbara, CA 93106, USA*

*E-mail: amsel@physics.ucsb.edu, marolf@physics.ucsb.edu, virmani@physics.ucsb.edu*

**ABSTRACT:** We use AdS/CFT to investigate *i*) high energy collisions with balls of deconfined plasma surrounded by a confining phase and *ii*) the rapid localized heating of a deconfined plasma. Both of these processes are dual to collisions with black holes, where they result in the nucleation of a new “arm” of the horizon reaching out in the direction of the incident object. We study the resulting non-equilibrium dynamics in a universal limit of the gravitational physics which may indicate universal behavior of deconfined plasmas at large  $N_c$ . Process (*i*) produces “virtual” arms of the plasma ball, while process (*ii*) can nucleate surprisingly large bubbles of a higher temperature phase.

**KEYWORDS:** Black Hole Collisions, Horizons, AdS/CFT.

---

## Contents

<b>1. Introduction</b>	<b>1</b>
<b>2. How far can a black hole reach?</b>	<b>3</b>
2.1 Physical and mathematical framework	3
2.2 Extraction of parameters	6
<b>3. Arm nucleation for plasma balls</b>	<b>9</b>
<b>4. Localized heating of deconfined plasmas</b>	<b>13</b>
4.1 Brief review: AdS/CFT with flavor	13
4.2 Bubbles of melted mesons	14
<b>5. Discussion</b>	<b>19</b>
<b>A. Brane dynamics in the Aichelburg-Sexl solution</b>	<b>21</b>

---

## 1. Introduction

Studies of gravity/gauge duality [1, 2, 3] have given insight into many aspects of strongly coupled gauge theories. A central aspect of this correspondence is that deconfined plasmas in the gauge theory are dual to black holes on the gravity side of the correspondence [3]. Although no gravity dual is known for gauge theories of direct experimental interest (e.g., QCD), the universal properties of black holes in gravity suggest that insights obtained from gravity/gauge duality may describe universal aspects of deconfined plasmas at large  $\lambda$ ,  $N_c$ , where  $N_c$  is the number of colors and  $\lambda$  is the 't Hooft coupling. The known utility of the large  $N_c$  expansion in QCD then further suggests that such dualities may help to explain the physics observed at heavy ion colliders [4, 5, 6, 7]. See e.g., [8] for a recent review.

Much of the literature on this subject has focused on using black holes to explore equilibrium thermodynamic properties of deconfined plasmas (such as entropies, free energies, and phase transitions, see e.g., [3, 9]) or quasi-static near-equilibrium properties such as hydrodynamic transport coefficients, see e.g., [4, 5, 6]. While transport coefficients can describe important hydrodynamics (such as elliptic flow, see e.g., [10]), such processes must be quasi-static in the sense that each local region of the plasma remains close to thermal equilibrium.

However, one may also ask about more dynamic processes. One example is the formation of a plasma from collisions studied in [7]. We will be interested here in related (but different) settings, involving the rapid transfer of energy to *pre-existing* plasmas. At low

rates of energy transfer, these processes result in a flow of heat described by hydrodynamic thermal conductivity, perhaps associated with some expansion or hydrodynamic flow of the plasma. But what happens at higher rates of energy transfer?

The result is most easily seen from the gravity dual. Recall that the most interesting feature of the dual black hole is its event horizon and that this horizon is a surface defined by null geodesics. A small energy flux across the black hole horizon leads only to local expansion of the horizon in a manner readily described by hydrodynamics (see e.g., [11]). On the other hand, larger fluxes lead to more dramatic results. As an extreme case, consider the collision of a small black hole with a larger black hole as shown in Fig. 1.

At first, the two black holes approach each other, each maintaining its own event horizon with only minor effects from the other black hole. However, when the black holes are sufficiently close together a new common horizon suddenly forms around both black holes, resulting in a single highly deformed black hole. In particular, the region between the two black holes is now enclosed in a new “arm” extending from the large black hole. The arm is then absorbed by the black hole as the system relaxes to equilibrium.

This picture is currently being investigated in numerical simulations of black hole collisions [12], though the analogous phenomenon for collisions of equal mass black holes is already well illustrated by numerical simulations, see e.g., [13]. In any case, it has long been known on general grounds (see e.g., [14, 15]) that the new arm of the horizon forms along a spacelike caustic; i.e., the new arm of the black hole effectively nucleates “from scratch.” Furthermore, the incident object need not be another black hole for this to occur; any sufficiently rapid flux of incoming energy results in the formation of a similar black hole arm that reaches out toward the incoming object. As discussed in [16] (which generalizes the arguments of [11]), in any spacetime dimension  $d$  the threshold for such nucleation to occur is<sup>1</sup>

$$\frac{E}{A} \sim \frac{T}{G_d}, \quad (1.1)$$

where  $E, A$  are the energy and transverse area of the incident object,  $T$  is the temperature of the target black hole,  $G_d$  is Newton’s gravitational constant, and we have set  $\hbar = 1$ .

The purpose of this paper is to calculate the shape of the nucleating arm and to interpret the results in terms of deconfined plasmas; we shall be less concerned with the final relaxation to equilibrium. As we discuss in more detail below, the formation of a black hole arm can correspond to either of two processes for the plasma, depending on the direction in which the arm extends. If the black hole arm reaches out along one of the gauge theory directions, then our process is naturally interpreted as the formation of a “virtual” arm of deconfined plasma catalyzed by the incident flux of energy. If, on the

<sup>1</sup>This result holds for a homogeneous object much smaller than the curvature scale at the black hole horizon whose cross-section transverse to the motion is round. The size of the object along the direction of motion does not affect the result so long as the collision takes place in less than the relaxation time  $1/T$  of the black hole.

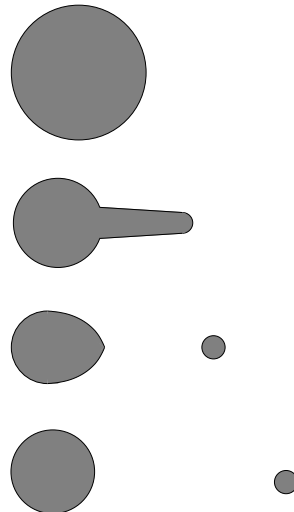


**Figure 1:** This cartoon depicts a time sequence of the creation of an “arm” as a small object falls into a large black hole. Note that the arm forms *before* the arrival of the incident object.

other hand, the black hole arm extends in the holographic direction (which corresponds to energy scales in the gauge theory), then it represents a strong local heating of the plasma via, for example, the decay of an excited quasi-particle of large mass<sup>2</sup>. Such heating takes the plasma far from local equilibrium and is not well-described by hydrodynamics. In particular, when the system allows further phase transitions, local heating can create a bubble of a higher temperature phase within the original plasma.

Though the details of specific models are certain to contain much interesting physics, our goal here is to take only the first steps toward understanding this dynamics in the context of gauge/gravity duality. For this reason, we focus here on universal or near-universal properties of collisions with black holes (and thus presumably with deconfined plasmas). In particular, we use the fact that the geometry sufficiently close to the horizon of any black hole of non-zero temperature can be approximated by Rindler space, which is just flat Minkowski space in accelerated coordinates. We also take the incident object to be both small and highly boosted so that horizon dynamics can be studied through the simple exercise of tracing null geodesics through the Aichelburg-Sexl metric [17].

This analysis is performed in section 2. We then interpret the results in terms of large  $N_c$  gauge theories in sections 3 and 4. Section 3 considers high energy collisions with plasma balls and the resulting virtual arms that extend in the gauge theory directions. Section 4 considers the case of rapid local heating. As a particular example we examine certain gauge theories with flavor in which stable mesons can exist within the original plasma. In that case, our local heating can cause the mesons to melt within a localized bubble, though the bubbles turn out to be surprisingly large. Gross properties of such bubbles are studied at both strong and weak 't Hooft couplings. We conclude with a brief discussion in section 5.

## 2. How far can a black hole reach?

In this section we address universal properties of collisions with black holes. Our primary goal is to characterize the black hole arm that nucleates to engulf an incident object. We wish to determine the shape of this arm, and in particular its thickness and length. Section 2.1 discusses the physical setup and determines the resulting horizon, while section 2.2 extracts the desired parameters.

### 2.1 Physical and mathematical framework

Our study of collisions with black holes is carried out under two key approximations, within which the behavior is universal. First, we use the fact that the geometry sufficiently close to the horizon of any black hole with temperature  $T \neq 0$  can be approximated by Rindler space, which is just flat Minkowski space in accelerated coordinates. Second, we consider the limit where the object approaches the black hole at high velocity so that generic (uncharged, non-spinning) objects are well-described by the simple Aichelburg-Sexl metric

---

<sup>2</sup>One can see from the gravity dual that such quasi-particles exist at large  $N_c, \lambda$  even in the deconfined phased. These quasi-particles correspond to bulk gravitons, strings, or localized black holes raised sufficiently far above the horizon of the black hole associated with the deconfinement transition.

[17]. Studying horizon dynamics during the collision then reduces to tracking null geodesics (the so-called generators of the event horizon) as they propagate through the associated spacetime. Such geodesics were studied in [18], which we review below for completeness.

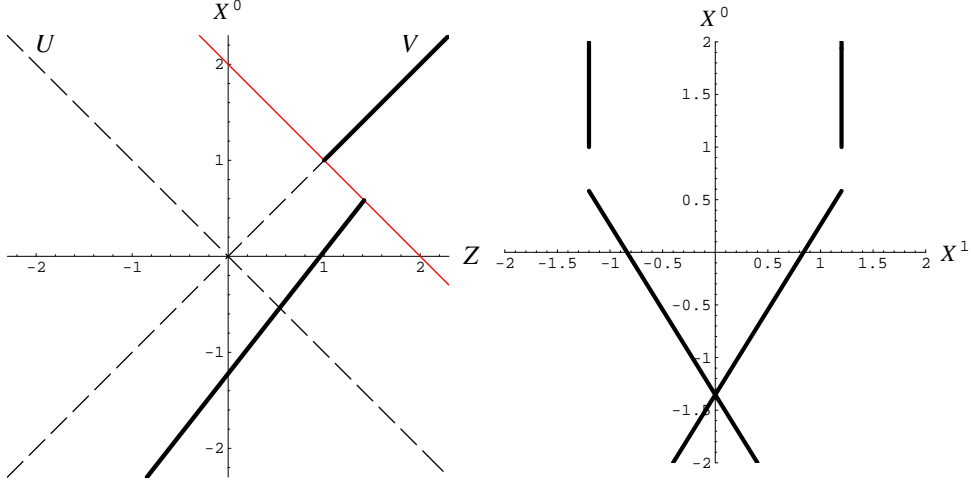


**Figure 2: Left:** Null geodesics (thick black lines) are shown projected into the  $Z, X^0$  plane. The geodesics experience a discontinuity when they reach the plane  $V = V_0$  of the Aichelburg-Sexl wave, shown as a thin line. The dashed lines are the  $U = 0$  and  $V = 0$  planes. In this example, the velocity component  $dZ/dX^0$  of the geodesic is positive both before and after the shift, but in general for  $V < V_0$  the velocity  $dZ/dX^0$  may be positive, negative, or zero depending on  $b$ . **Right:** Null geodesics are shown projected into the  $X^1, X^0$  plane. Below  $V = V_0$ , the geodesics focus toward  $X^1 = 0$ . Both figures show  $b = 1.2$ ,  $c_d \mu = 1$ ,  $V_0 = 2$ , and  $d = 5$ .

We consider the general case of  $d \geq 4$  spacetime dimensions. In light-cone coordinates  $V = X^0 + Z$ ,  $U = X^0 - Z$  the Aichelburg-Sexl metric [17] takes the form

$$ds^2 = -dUdV + d\rho^2 + \rho^2 d\Omega_{d-3}^2 + \mu\Phi(\rho)\delta(V - V_0)dV^2, \quad (2.1)$$

where we have defined  $\rho^2 = (X^1)^2 + \dots + (X^{d-2})^2$ . Here the incident mass moves in the negative  $Z$  direction at  $\rho = 0$  within the null plane  $V = V_0$ . Note that, due to the delta-function above, the metric differs from flat Minkowski space only within this null plane. The result (2.1) can be obtained from the mass  $m$  Schwarzschild metric in  $d$  dimensions by Lorentz transforming to a frame in which the particle travels with speed  $v$ . In units where  $c = 1$ , one then takes the limits  $m \rightarrow 0$  and  $v \rightarrow 1$  in such a way that the quantity  $\mu = m(1 - v^2)^{-1/2}$  appearing in (2.1) remains constant.

The Aichelburg-Sexl potential<sup>3</sup> appearing in (2.1) is given by

$$\Phi(\rho) = \begin{cases} -c_4 \ln\left(\frac{\rho}{\rho_0}\right) & \text{if } d = 4 \\ \frac{c_d}{(d-4)\rho^{d-4}} & \text{if } d > 4 \end{cases}, \quad (2.2)$$

<sup>3</sup>In contrast to the usual convention, we have separated the factor of  $\mu$  from the rest of the potential in order to make  $\Phi(\rho)$  boost-invariant.

where

$$c_d = \frac{16\pi G_d}{\Omega_{d-3}}, \quad (2.3)$$

$\Omega_n$  denotes the volume of  $S^n$ , and the length scale  $\rho_0$  is an arbitrary gauge choice. Note that the potential  $\Phi(\rho)$  solves Poisson's equation in  $d-2$  dimensions with a point source.

The Aichelburg-Sexl solution will accurately describe the metric for  $\rho \geq r$ , where  $r$  is the transverse size of the incident object. The metric for  $\rho < r$  depends on the internal structure of the object; we will ignore the details in this region and treat  $\rho \sim r$  only as a cut-off on the singularity of  $\Phi$ . To describe a beam of incident objects, this point source would be replaced by a line, or by a line segment for a pulsed beam. We consider here only the point source case (2.2), or equivalently the limit of short pulse duration  $\Delta t \ll 1/T$ .

In the Rindler approximation, the black hole time-translation is the boost generator  $\chi = 2\pi T(V\partial_V - U\partial_U)$ , where we have used the fact that the so-called surface gravity  $\kappa$  which determines the normalization of the boost generator is related to the black hole temperature through  $\kappa = 2\pi T$  in units with  $\hbar = c = 1$ . Thus the energy of the incident object is

$$E = -\chi_\nu p^\nu = 2\pi\mu T V_0. \quad (2.4)$$

We wish to use the above metric to locate the (future) black hole event horizon, which as always is determined by a boundary condition in the far future. Since (2.1) is precisely the Minkowski metric for  $V > V_0$ , the horizon there must agree with some null plane; i.e., with a Rindler horizon. We take this null plane to be  $U = 0$ . The past horizon of the black hole is similarly determined by a boundary condition in the far past; we take this horizon to lie at  $V = 0$ . Having established the boundary conditions, we need only trace the relevant null geodesics back from the far future through the shock wave at  $V = V_0$  to find the full horizon. We may think of this as calculating the deviation of the true event horizon from the unperturbed event horizon at  $U = 0$ .

The geodesic equation

$$\frac{d^2 x^\nu}{d\lambda^2} + \Gamma_{\rho\sigma}^\nu \frac{dx^\rho}{d\lambda} \frac{dx^\sigma}{d\lambda} = 0 \quad (2.5)$$

was studied for (2.1) in [18] and it is instructive to review their calculation. Setting the index  $\nu = V$  in (2.5) reveals that  $V$  is an affine parameter, so henceforth we will set  $\lambda = V$ . Setting  $\nu = \rho$  then yields

$$\frac{d^2 \rho}{dV^2} - \frac{\mu}{2} \frac{d\Phi}{d\rho} \delta(V - V_0) = 0, \quad (2.6)$$

while  $\nu = U$  leads to

$$\frac{d^2 U}{dV^2} - \mu\Phi(\rho) \frac{d}{dV} \delta(V - V_0) - 2\mu \frac{d\Phi}{d\rho} \frac{d\rho}{dV} \delta(V - V_0) = 0. \quad (2.7)$$

These equations are solved by

$$\rho(V) = b + \mu \frac{\Phi'(b)}{2} (V_0 - V) \Theta(V_0 - V), \quad (2.8)$$

$$U(V) = \mu^2 \frac{\Phi'(b)^2}{4} (V - V_0) \Theta(V_0 - V) - \mu\Phi(b) \Theta(V_0 - V), \quad (2.9)$$

where we have chosen boundary conditions such that far in the future (i.e.,  $V > V_0$ ) we have  $\rho \rightarrow b$ ,  $U \rightarrow 0$  (see Fig. 2). It is straightforward to check that  $ds^2 = 0$  along such curves, so these are indeed null geodesics.

For  $V > V_0$ , the geodesics are straight lines of constant  $\rho$  in the  $U = 0$  plane. When a geodesic of given impact parameter  $\rho = b$  reaches  $V = V_0$ , there is a discontinuous jump<sup>4</sup> in  $U$  given by  $\Delta U = -\mu\Phi(b)$ , where the sign corresponds to tracing the geodesics backwards from  $V = \infty$ . For  $d > 4$ , we have  $\Delta U < 0$ , and  $\Delta U \rightarrow 0$  as  $b \rightarrow \infty$ . This is not the case for  $d = 4$  due to a logarithmic divergence.

Below the discontinuity our null geodesics are once again straight lines, but since

$$\frac{d\rho}{dX^0} = -\mu \frac{\Phi'(b)}{1 + \frac{\mu^2 \Phi'(b)^2}{4}} > 0 \quad \text{for } V < V_0, \quad (2.10)$$

they now begin to focus toward  $\rho = 0$  (Fig. 2). All geodesics with impact parameter  $b$  intersect at a common point, and the set of such intersections traces out a caustic as a function of  $b$ . Physically, this caustic describes the nucleation of the event horizon.

From (2.8) and (2.9) we see that the caustic occurs at

$$V_c = V_0 + \frac{2b}{\mu\Phi'(b)} \quad (2.11)$$

$$U_c = -\mu\Phi(b) + \frac{b\mu}{2}\Phi'(b). \quad (2.12)$$

This curve is plotted in Fig. 3. We have distinguished the  $V < 0$  and  $V > 0$  parts of the caustic, as only the  $V > 0$  part of the spacetime is physically relevant; the rest is hidden behind the past horizon. Since geodesics with large  $b$  emerge from the past horizon, we will refer to them as forming the “body” of the event horizon, while geodesics with small  $b$  intersect the caustic at  $V > 0$  and form the “arm” of the horizon described in the introduction. We see from Fig. 3 that the caustic along which the arm nucleates approaches the world line of the incident object in the limit  $b \rightarrow 0$ . Thus the arm reaches out in the direction from which the object is incident by an amount that depends on the cut-off  $r$ .

## 2.2 Extraction of parameters

Within our approximations, the above equations determine the shape of the horizon and

<sup>4</sup>A  $\rho$ -independent relative shift of the regions above and below  $V = V_0$  is a gauge transformation which changes  $\Delta U$  by a constant. It is in this sense that  $\rho_0$  in (2.2) is a gauge parameter for  $d = 4$ . In contrast, the  $\rho$ -dependent part of  $\Delta U$  is a physical effect [19] describing the integrated relative shift of geodesics passing through the shock wave. Were the delta function in (2.1) replaced by a smooth function of compact support, the geodesics would become continuous but would still experience a net displacement  $\Delta U$  as they traverse the shock.

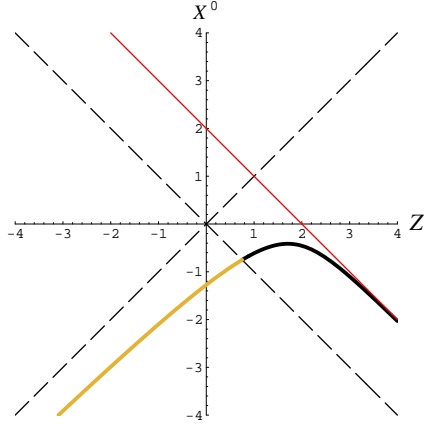


**Figure 3:** The caustic is shown in the  $Z, X^0$  plane for  $c_d\mu = 1$ ,  $V_0 = 2$ , and  $d = 5$ . For  $b > b_*$ , the caustic is hidden behind the past horizon. For  $b < b_*$  (black segment) the caustic lies above the past horizon. This portion of the caustic nucleates the “arm” of the black hole.

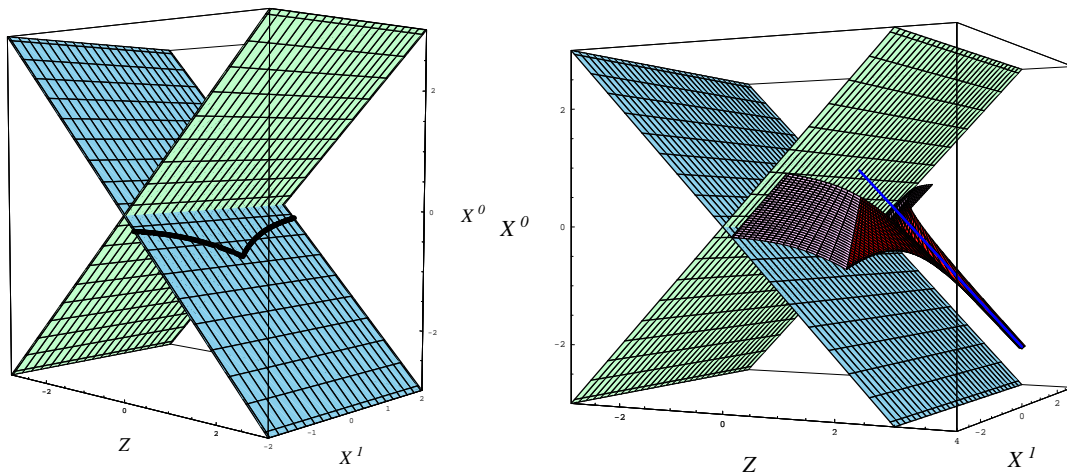


**Figure 4:** **Left:** The distortion of the body of the horizon by the gravitational field of the incoming object. The curve shows where geodesics with  $b > b_*$  intersect the past horizon. The cusp corresponds to  $b = b_*$ , where the caustic intersects the past horizon. **Right:** The body ( $b > b_*$ , lighter part of the curved surface) and arm ( $b < b_*$ , darker part of the curved surface) of the horizon. The surface shown is generated by geodesics for a range of impact parameters  $b$ . The portion of the surface above the caustic and with  $V < V_0$  is shown. For small  $b$  the spacelike curve of caustics from which the arm nucleates is seen to approach the line ( $V = V_0, X^i = 0$ ) showing the path of the incoming particle. Both figures show  $c_{d\mu} = 1$ ,  $V_0 = 2$ , and  $d = 5$ .

the newly-nucleated arm. We now extract parameters describing the various length scales involved for use in our discussion of deconfined plasmas. Since both body and arm are dynamical objects, their lengths (and widths) will be functions of time or, more generally, of the spacetime surface on which they are measured. We will make certain natural choices below.

Let us begin with the body of the future event horizon, which consists of geodesics that emerge from the past horizon. The point where a given geodesic intersects the unperturbed past horizon is given by setting  $V = 0$  in (2.8) and (2.9). The corresponding curve is plotted in Fig. 4 (left), and shows the distortion (at the past horizon) of the black hole body by the incoming flux of energy. For  $d > 4$ , geodesics with large  $b$  experience only a small deflection, and the body at large  $b$  approaches the unperturbed event horizon. The cusp in Fig. 4 (left) is the event at which the caustic emerges from the past horizon. It is described by  $V_c = 0$  in (2.11) and thus by impact parameter<sup>5</sup>

$$b_* = \left( \frac{4G_d E}{\Omega_{d-3} T} \right)^{\frac{1}{d-2}}. \quad (2.13)$$

Both the evolution of the body and the nucleation of the arm can be seen (Fig. 4 (right)) by plotting the geodesics for many values of  $b$ .

We now extract some relevant length scales describing the deformation of the unperturbed horizon, including the length of the arm. One useful measure of distance is the

<sup>5</sup>The result  $b_* \sim (E/T)^{\frac{1}{d-2}}$  is quite general and does not depend on the use of the Aichelburg-Sexl approximation. See [16].



proper distance from the surface  $U = 0, V = 0$  where the unperturbed horizons intersect. Surfaces of constant proper distance contain the worldlines of static observers outside the unperturbed black hole. These surfaces are just hyperbolae in the Minkowski coordinates  $(X^0, Z)$  satisfying

$$Z^2 - (X^0)^2 = -UV = a^2 \quad (2.14)$$

for some constant  $a$ .

We can ask which of these hyperbolae intersect a geodesic with given impact parameter  $b$ , though we must take some care due to the jump across the Aichelburg-Sexl plane. Let  $P$  denote the point on the geodesic immediately below the shift, so that  $U(P) = -\mu\Phi(b)$ ,  $V(P) = V_0$ . There are two cases: In the first case,  $dZ/dX^0$  at  $P$  is greater for the geodesic than for a surface of constant  $a$ . In this case the geodesic is at  $a < a(P)$  for  $V < V_0$  and we may say that this part of the horizon extends precisely to  $a(P)$ . This occurs at large  $b$ , say  $b > \hat{b}$ . In the second case ( $b < \hat{b}$ ), one finds that  $dZ/dX^0$  at  $P$  is less for the geodesic than for a surface of constant  $a$ . In this case, the extension of the horizon in the  $Z$  direction is characterized by the value  $a$  associated with the hyperbola tangent to the geodesic below  $P$ . The two cases are shown in Fig. 5.

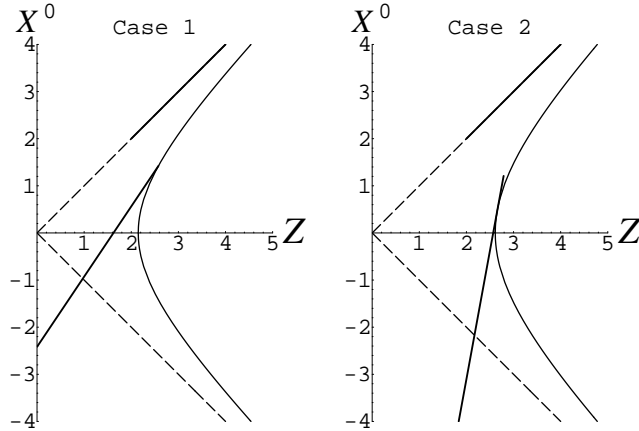


**Figure 5:** Null geodesics and some hyperbolae for constant  $a$  are shown for  $c_d = 1.5$ ,  $V_0 = 4$ , and  $d = 5$ . Case 1: For  $b$  sufficiently large (e.g.,  $b = 1.3$ ), the desired hyperbola intersects the geodesic at the point  $P$ , that is, immediately after the shift. Case 2: If  $b$  is smaller than some critical value (e.g., for  $b = 0.95$ ), the geodesic is tangent to the desired hyperbola at a point with  $V < V_0$ .

We restrict our analysis to the case  $d > 4$ , where the perturbed horizon asymptotically approaches  $U = 0$  so that there is a well-defined asymptotic bifurcation surface from which to measure proper distance. The results are:

$$\begin{aligned} \text{Case 1: For } b > \hat{b} \quad a &= a(P) = \sqrt{\frac{8G_d E}{(d-4)\Omega_{d-3} b^{d-4} T}}, \\ \text{Case 2: For } b < \hat{b} \quad a &= \frac{b}{d-4} + \frac{2G_d E}{\Omega_{d-3} T b^{d-3}}. \end{aligned} \quad (2.15)$$

where  $\hat{b}$  is given by

$$\hat{b} = \left(\frac{d-4}{2}\right)^{\frac{1}{d-2}} b_* = \left(\frac{d-4}{2}\right)^{\frac{1}{d-2}} \left(\frac{4G_d E}{\Omega_{d-3} T}\right)^{\frac{1}{d-2}}. \quad (2.16)$$

The maximum extension (or length) of the arm<sup>6</sup> is just (2.15) evaluated at the cut-off  $b = r$ . Note that for  $d \geq 6$  any geodesic intersecting the arm satisfies  $b \leq b_* \leq \hat{b}$ , so that case 2 always applies. Even for  $d = 5$ , case 2 applies whenever the effect is significant,  $r \ll b_*$ . In this limit one finds

$$L_{BH \text{ arm}} \approx \frac{2G_d E}{\Omega_{d-3} T r^{d-3}}. \quad (2.17)$$

We note once again that, due to the Rindler approximation, this result is justified only in cases where  $L_{BH \text{ arm}}$  is smaller than the characteristic curvature scale of the spacetime near the horizon.

We may also characterize the arm by its width in the Aichelburg-Sexl plane. At each  $U$  this width is just the impact parameter, which ranges from  $b_* = \left(\frac{4G_d E}{\Omega_{d-3} T}\right)^{\frac{1}{d-2}}$ , where the arm connects to the body, to the cut-off  $r$  at the tip.

### 3. Arm nucleation for plasma balls

In gauge/gravity duality, balls of deconfined plasma surrounded by a confining phase are dual to black holes that are localized in the gauge theory directions. Such black holes naturally have temperature  $T = T_d$ , where  $T_d$  is the temperature of the deconfinement phase transition [20]. A particle incident on the gauge theory plasma ball corresponds to a flux of energy incident on the black hole. If this flux is large enough, the black hole may nucleate an arm as described in section 2.

How precisely should we understand the corresponding effect in the gauge theory? In some sense the plasma ball must also nucleate an arm along the path of the incoming particle. What is interesting is that Fig. 4 (right) indicates that this nucleation occurs *in front* of the incoming particle; i.e., before the particle arrives.



**Figure 6:** A particle incident on a black hole dual to a ball of deconfined plasma.

Such behavior may appear to be acausal, but the same words might be applied to the nucleation of the arm on the black hole. Yet the physics of the black hole arm is clear. Gravity propagates causally, and the spacetime in the region of the arm has no locally measurable differences from the spacetime outside. It is the fact that one traces the event horizon backwards from the far future that allows the arm to form before the particles arrive. In other words, our designation of the arm as being “part” of the black hole describes the fact that, due to the imminent arrival of the incident energy, the gravitational interactions *will* become large enough that no information from the arm-like region will be able to escape to infinity.

<sup>6</sup>In the regime of most interest,  $r \ll b_*$ , the contribution from the black hole body is negligible in comparison to the length of the black hole arm, so henceforth we will refer to the “maximum extension of the arm” as simply the “length of the arm.”

This suggests a straightforward interpretation of the corresponding “arm” of the plasma ball: Due to causality, the arm is locally indistinguishable from the confining vacuum. In particular, its energy density remains that of the vacuum and the arm contains no plasma. Instead, the arm marks a region of spacetime in which any additional particle has a large probability to be caught up in the interactions that *will* ensue and thus to fuse with the plasma ball. In effect, the arm describes a temporary and highly anisotropic enlargement of the capture cross-section associated with the plasma ball. To remind the reader of this interpretation, we will henceforth refer to such arms as “virtual” in the context of plasma balls.

Now, even without the nucleation of virtual arms, the capture cross-section for particles incident from infinity will be somewhat larger than the size of the plasma ball itself. Recall, for example, that while the event horizon for the familiar static Schwarzschild black hole lies at area-radius  $2G_4M$ , any free particle passing within the sphere of area-radius  $3G_4M$  is necessarily captured by the black hole. It is thus clear that there will be a similar effect in the gauge theory dual<sup>7</sup>.

However, the arm describes a region of spacetime tied even more strongly to the plasma ball. Suppose that two additional (probe) beams are aimed so as to collide near the plasma. If the interaction region lies outside the virtual arm, then some of the debris from the interaction can escape to infinity. However, when an interaction takes place inside the virtual arm, *all* of the particles produced in the collision will have large amplitudes to fuse with the plasma ball and no signal will reach an external detector. This difference is illustrated in Fig. 7.

One may hope to one day observe the effects of similar virtual arms in experiments with deconfined QCD plasmas. In this context, recall that our description of black hole arms in section 2 is universal in the limit of *i*) high velocity collisions and *ii*) studying the region near the black hole. As a result, experiments that probe plasmas in the corresponding regime can provide a new universal test of the extent to which such plasmas admit a dual description by *any* semi-classical gravity system, without first needing to propose a particular dual theory.

<sup>7</sup>Our Rindler-space near-horizon approximation is enough to predict that any low-mass particle incident from infinity is captured as long as it approaches within some distance of order the curvature scale of the spacetime near the horizon. However, the full capture cross-section may well be even larger.

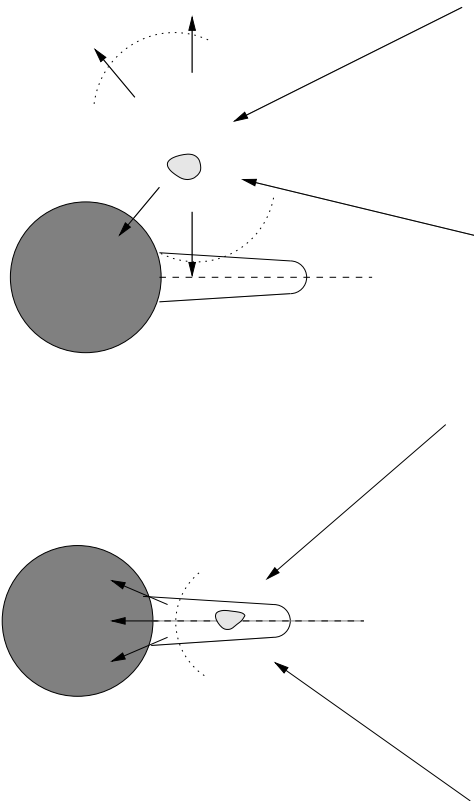


**Figure 7: Top:** Particles produced in a collision exterior to the virtual arm can reach the detector. **Bottom:** Particles produced in a collision inside the virtual arm fuse with the plasma ball and will not be detected far away.

To illustrate this idea, let us consider the length of the arm (2.17), which describes the limit of large velocity for the incident particles. We wish to translate this result into a length  $L_{plasma\ arm}$  for the arm of virtual plasma measured in gauge theory units. Since (2.17) contains a factor of  $G_d$ , and since the relation between  $G_d$  and the gauge theory parameters is model-dependent, the result will no longer be completely universal. However, the scaling of  $L_{plasma\ arm}$  with various parameters describing the incident particle will be universal. Precise predictions can of course be obtained for particular models; we give an example at the end of this section.

The main task is to determine how distances (such as  $r$ ,  $L_{BH\ arm}$ ) in the gravity description are related to gauge theory distances. Here the high symmetry of our near-horizon limit is quite useful. Recall that we consider regions close enough to the horizon to regard the surface as flat. Thus we have Euclidean symmetry along the horizon as well as translation symmetry in time. There is also a reflection symmetry which inverts any constant  $z$  surface through any point on that surface. As a result, in terms of the coordinates  $\rho, z, t$  the gauge theory metric must be of the form

$$ds_{YM}^2 = \sigma^2(z) (-f(z)dt^2 + g(z)dz^2 + d\rho^2 + \rho^2 d\Omega_{D-3}^2) , \quad (3.1)$$

where we have taken the gauge theory to live in  $D$  dimensions. In addition, the original coordinate  $t$  was normalized to the unit time-translation in the gauge theory. Thus,  $f = \sigma^{-2}$ . Since the gauge theory space-translation (say, in the transverse directions) also has constant norm,  $\sigma$  must be a constant. The gauge theory metric is thus

$$ds_{YM}^2 = -dt^2 + \sigma^2 (g(z)dz^2 + d\rho^2 + \rho^2 d\Omega_{D-3}^2) . \quad (3.2)$$

Any such metric describes flat Minkowski space (as desired), but the particular form of (3.2) tells us how to translate our bulk coordinates into gauge theory terms.

Information about  $g(z)$  may now be obtained by considering the energy of strings stretched in both gauge theory and bulk. First recall that (2.17) was obtained in the limit where one is close enough to the black hole horizon to approximate the metric by the Rindler metric,

$$ds^2 = -(2\pi T_d)^2 z^2 dt^2 + dz^2 + d\rho^2 + \rho^2 d\Omega_{d-3}^2 . \quad (3.3)$$

Now consider a bit of string located near the horizon and oriented parallel to the horizon, that is, at constant  $z$ . If, for example, such a string were stretched in the  $\rho$  direction (at fixed angles) with coordinate extent  $\Delta\rho$ , then its energy would be  $E = \ell_s^{-2} T_d z \Delta\rho$ . Far from the plasma ball, the energy of the corresponding stretched string in the gauge theory would be  $E = (2\pi\alpha')^{-1} (\sigma\Delta\rho)$  where  $\alpha'$  is the gauge theory Regge slope. However, these two expressions cannot be equal as the gauge theory expression does not depend on  $z$ . The point here is that there is an attractive force between the string and the plasma ball, so that proximity to the plasma ball changes the effective string tension (and thus the effective Regge slope) by a  $z$ -dependent shift in the tension.

Let us call the effective Regge slope  $\beta(z)\alpha'$ . Setting the resulting energies equal yields  $\frac{\sigma}{\beta} = \frac{2\pi\alpha' T_d z}{\ell_s^2}$ . If we assume that the renormalization factor  $\beta$  depends only on  $z$  and not on

the orientation of the string, we may obtain information about  $g(z)$  by considering bits of string stretched in the  $z$ -direction:

$$\ell_s^{-2} T_d z \Delta z = E = \frac{1}{2\pi\beta\alpha'} \sigma(\sqrt{g}\Delta z), \quad \text{or } g = 1. \quad (3.4)$$

This implies that spatial distances are merely rescaled by a factor of  $\sigma$  when passing from gravity to gauge theory measurements. Thus, the size of the incident object in the gauge theory is  $\tilde{r} = \sigma r$  and the length of the virtual plasma arm is

$$L_{\text{plasma arm}} \approx \frac{2\hat{G}_d \hat{\sigma}^{d-2} \alpha'^{\frac{d-2}{2}} E}{N_c^2 \Omega_{d-3} T_d \tilde{r}^{d-3}}, \quad (3.5)$$

where  $\hat{G}_d$  and  $\hat{\sigma}$  are defined by  $\hat{G}_d = N_c^2 G_d / \ell_s^{d-2}$  and  $\hat{\sigma} = \sigma \left( \frac{\ell_s^2}{\alpha'} \right)^{1/2}$ . We conclude that the length of the virtual arm scales with the energy of the incident particle and inversely with a power of the particle's characteristic size. This power determines the effective dimension of the gravity dual. Similarly, the width of the arm ranges from  $W_{\text{plasma arm}}^{\text{max}} = \hat{\sigma} \alpha'^{1/2} \left( \frac{4\hat{G}_d E}{N_c^2 \Omega_{d-3} T_d} \right)^{\frac{1}{d-2}}$  where it connects with the plasma ball to  $W_{\text{plasma arm}}^{\text{min}} = \tilde{r}$  at the tip.

It is clear that  $\hat{G}_d$  is a dimensionless model-dependent function; i.e., a function of  $\lambda$ . To clarify the nature of  $\hat{\sigma}$ , let us first consider  $\sigma = 2\pi\beta\alpha' T_d z / \ell_s^2$ . For a given plasma ball, we already know that  $\sigma$  is a dimensionless constant summarizing the scale of gauge theory proper distances relative to gravity proper distances near the black hole. On the other hand, far from the black hole the scale factor relating gauge theory relative to gravity distances is just  $\left( \frac{\alpha'}{\ell_s^2} \right)^{1/2}$ . Thus,  $\hat{\sigma} = \sigma \left( \frac{\ell_s^2}{\alpha'} \right)^{1/2}$  gives precisely the scale factor of gravity distances near the black hole relative to those far away; i.e., it is determined by the black hole metric. As a property of a classical solution of a pure gravity theory,  $\hat{\sigma}$  cannot depend on  $G_d$ , and must be a function only of  $L/R$ , where  $R$  is the size of the black hole and  $L$  is the AdS scale. Let us, however, consider the relation  $\hat{\sigma} = \left( \frac{\ell_s^2}{\alpha'} \right)^{1/2} \sigma = 2\pi\beta\alpha'^{1/2} T_d z / \ell_s$  from the gauge theory point of view. (In terms of the gauge theory proper distance  $\tilde{z} = \sigma z$  this is  $\hat{\sigma}^2 = 2\pi\beta T_d \tilde{z}$ .) The only factor through which the size of the black hole (i.e., the size of the plasma ball) might enter is  $\beta$ , the renormalization of the Regge slope. But since this renormalization is due to interactions with the plasma ball, at small  $\tilde{z}$  (small separation from the plasma ball) one expects  $\beta$  to depend only on  $\tilde{z}$  and to become independent of  $R$ . Thus we deduce that  $\hat{\sigma}$  is in fact a constant of order one which depends only on qualitative features of the model. From the gravity perspective this means that  $\hat{\sigma}$  is independent of  $G_d, L, R$ , while from the gauge theory perspective  $\hat{\sigma}$  is independent of  $\lambda, N_c, \alpha'$ .

A particular gauge/gravity duality of this kind was considered in [3, 20]. There a (2+1) dimensional theory was obtained by taking the low energy limit of  $\mathcal{N} = 4$  super Yang-Mills compactified on a Scherk-Schwarz spatial circle. This theory is dual to a IIB supergravity system whose ground state is the Cartesian product of the AdS soliton [21] and  $S^5$ . In the  $\lambda \rightarrow 0$  limit, the field theory is pure (2+1) Yang Mills [3]. At large  $\lambda$ , where the classical gravity description is valid, the gauge theory is unfamiliar. Nevertheless,

it was conjectured in [20] that finite mass black holes have a dual description in this theory in terms of localized lumps of deconfined plasma. If the incident particle has no  $R$ -symmetry charge, the corresponding object in the gravity dual is delocalized on the  $S^5$  so that the effective dimension is  $d = 5$  and (using the conventions of section 4.1 below)  $\hat{G}_5 = 2^{-1/4}\pi\lambda^{3/4}$ .

One would also like to determine the constant  $\hat{\sigma}$  for this model. In principle, this can be read off from the bulk metric which describes the domain-wall limit considered in [20] (where the black hole fills a half-plane). In that case  $\hat{\sigma} = |k|_\infty/|k|_{BH}$ , where  $|k|_\infty$  is the norm of a translational Killing field  $k$  along the domain wall evaluated far from the black hole but on the IR floor of the spacetime and  $|k|_{BH}$  is the norm of  $k$  evaluated near the horizon of the black hole. Using Fig. 6 of [20], it is reasonable to estimate that  $\hat{\sigma} \approx 1$ .

## 4. Localized heating of deconfined plasmas

Section 3 above discussed the gauge theory dual of a process in which a high-velocity object is incident on the black hole from a gauge theory direction. However, another interesting setting occurs when the object is incident on the black hole from the holographic direction. In this case, the incident object represents a localized heating of the plasma, perhaps due to the decay of massive quasi-particles (see section 4.2 below).

If the theory has additional phase transitions above the deconfinement temperature  $T_d$ , then this local heating can induce the formation of a bubble of the high temperature phase. We now study such bubble formation and the ensuing bubble dynamics in a particular gauge/gravity correspondence.

### 4.1 Brief review: AdS/CFT with flavor

Recall [22, 23] that in AdS/CFT, a small number of flavors ( $N_f \ll N_c$ ) of fundamental matter (“quarks”) may be described by probe D-branes in a background AdS space. The transverse displacement of the probe branes from the D3-branes that describe AdS space sets the mass of the quarks. We consider the case where the bulk solution contains a black hole at temperature  $T$ . Although the probe branes are attracted to the black hole, at high enough quark mass the tension of the branes is sufficient to balance this attractive force and the probe branes lie outside the horizon in what is often called a ‘Minkowski’ embedding [24, 25]. In this phase, the gauge theory contains stable mesons with a discrete mass spectrum. However, above a critical temperature  $T_f$ , the gravitational force overcomes the tension and the probe branes fall through the horizon. The associated embeddings are referred to as ‘black hole’ embeddings. In this phase, the gauge theory has no stable mesons; the mesons melt. A detailed thermodynamic analysis of these embeddings reveals that the system undergoes a first order phase transition at  $T = T_f$ , where the probe branes jump discontinuously from a Minkowski to a black hole embedding [24, 25].

This phase transition has been studied extensively in systems of  $N_f$  probe D7-branes in the background of  $N_c$  black D3-branes, with  $N_f \ll N_c$ . Without the D7-branes, the system is conformal and does not confine. Nevertheless, it can be a good model of a

confining system at sufficiently high temperatures  $T \gg T_d$ . We now specialize to this model and fix the notation to be used below.

The background metric for the black D3-branes may be written

$$ds^2 = \left(\frac{u}{L}\right)^2 (-f dt^2 + d\vec{x}^2) + \left(\frac{L}{u}\right)^2 \left(\frac{du^2}{f} + u^2 d\Omega_5^2\right), \quad (4.1)$$

where  $f = 1 - (u_0/u)^4$ . The gauge theory directions are  $\vec{x} = (x^1, x^2, x^3)$ , and the line element of the  $S^5$  is

$$d\Omega_5^2 = d\theta^2 + \sin^2 \theta d\Omega_3^2 + \cos^2 \theta d\phi^2. \quad (4.2)$$

The length scale  $L$  can be expressed as

$$L^4 = 4\pi g_s N_c \ell_s^4 = 2\lambda \ell_s^4, \quad (4.3)$$

where  $g_s$  is the string coupling,  $\ell_s$  is the string length, and we have defined the 't Hooft coupling  $\lambda = 2\pi g_s N_c$ . The horizon is at  $u = u_0$ , which is related to the temperature  $T$  through

$$T = \frac{u_0}{\pi L^2}. \quad (4.4)$$

As shown in [24, 25], the critical temperature for the meson melting phase transition is

$$T_f \sim \bar{M} \sim \frac{2M_q}{\sqrt{\lambda}}, \quad (4.5)$$

where  $\bar{M}$  characterizes the meson mass gap at temperatures well below the phase transition, the quark mass is  $M_q \sim u_0/\ell_s^2$ , and factors of order one have been neglected.

Now, in the near horizon limit, the metric (4.1) can be written in the standard Rindler form by defining the coordinates

$$\pi T z^2 = u - u_0, \quad y = L\theta, \quad (4.6)$$

and rescaling  $\vec{x} \rightarrow \frac{u_0}{L}\vec{x}$ . Then in the limit of small  $z$  and small  $y$ , the background metric becomes

$$ds^2 = -(2\pi T)^2 z^2 dt^2 + dz^2 + d\vec{x}^2 + dy^2 + y^2 d\Omega_3^2 + dx_9^2, \quad (4.7)$$

where  $\vec{x} = (x^1, x^2, x^3)$ . For further details we refer the reader to [24, 25, 26].

## 4.2 Bubbles of melted mesons

Consider now a thermal state of the gauge theory at some temperature  $T$  near  $T_f$  but satisfying  $T_f > T$ . The probe branes in the gravity dual lie on a Minkowski embedding which we may characterize by the minimum height  $z_0$  of the branes above the black hole. This minimum height occurs at  $y = 0$  and is related to the constituent and bare quark masses  $M_c, M_q$  through [25]

$$M_c \sim \frac{u_0 z_0^2}{\ell_s^2 L^2} \sim \frac{z_0^2}{L^2} M_q. \quad (4.8)$$

The constituent mass  $M_c$  is the physical quark mass taking into account thermal corrections.

From [25] we see that Minkowski embeddings with  $z_0 < 0.15L$  are thermodynamically unstable and will transition to black hole embeddings. Thus  $z_0 \gtrsim 0.15L$ . However, we wish to use the Rindler-space approximation (4.7), which neglects terms in the metric of order

$$\frac{u - u_0}{u_0} \sim \left(\frac{z}{L}\right)^2.$$

Thus for  $z \sim 0.15L$ , the error is of order  $(0.15)^2$ . This occurs when  $T$  is close to  $T_f$ . While not parametrically small, the above error is certainly not large and we expect that the Rindler approximation should correctly capture much of the physics. Below, we restrict attention to such cases (which implies  $M_c \sim (0.15)^2 M_q$ ) and use the Rindler approximation without further comment.

Suppose that we now perturb this equilibrium by adding a massive quasi-particle which would have been stable (or at least very long lived) at  $T = 0$ . In the presence of the thermal bath all such quasi-particles become unstable and decay, but at least at large  $\lambda, N_c$  some massive quasi-particles have lifetimes  $\Delta\tau$  much greater than their inverse masses  $m^{-1}$ . In the gravity dual such resonances merely correspond to raising some object (graviton, massive string state, or black hole) to a height  $z \gg z_0$  above the black hole horizon. We take the wave-function of this excitation in the gauge theory directions to be a Gaussian wave-packet centered on zero momentum with small width in momentum space, so that any spreading of the wave-packet is very slow. Due to the object's large mass, such wave-packets may nevertheless also be well-localized in position space.

Since our object was raised to a large height  $z$ , it quickly begins to fall. By the time it reaches  $z \sim z_0$ , the object is moving very rapidly. We restrict attention to an object which remains well-localized in the gauge theory directions (i.e., a beam-like graviton wave-packet directed downward, a massive string, or a small black hole), so that we may approximate its effect on the probe brane by that of an Aichelburg-Sexl shock wave of the form discussed in section 2 above.

Now, there are two settings that one might consider, depending on whether the object is localized or delocalized on the  $S^5$ . In the particular model considered here, the  $S^5$  has size of order  $L$ . Due to various dynamical instabilities such as the Gregory-Laflamme instability for black holes [27], one expects stable objects that are well-localized in the gauge theory directions and which satisfy  $r \ll L$  to also be well-localized on the  $S^5$ .

However, this fact means that the wavefunction of such objects will have components with significant charge under the  $SO(6)$   $R$ -symmetry associated with this sphere. If one eventually wishes to model more QCD-like systems without an  $R$ -symmetry, then one may expect that the case without  $R$ -charge provides more universal results. Thus, despite the fact that such solutions are unstable in our model, we concentrate below on Aichelburg-Sexl-like solutions which are homogeneous over the  $S^5$ .

In our Rindler-space near-horizon limit, this  $S^5$  is merely the  $\mathbb{R}^5$  spanned by  $y, \Omega_3, x^9$ . One may think of the resulting shock-wave solution as being described by a  $d = 5$  Aichelburg-Sexl solution (2.1) at each constant value of  $y, \Omega_3, x^9$ . In the notation of section 2 above, one may simply take the transverse radial coordinate to be  $\rho^2 = \vec{x}^2$  and  $d = 5$ .



We found previously that null geodesics undergo a discontinuous shift when they reach the plane of the shock. In fact, the same is true of any worldline subject to finite forces, as such forces add only a finite right-hand side to equation (2.5). Since the shift diverges at  $\rho = 0$ , it takes at least a portion of the D7-branes' worldvolume behind the black hole horizon. A localized bubble of the melted meson phase has been formed.

We wish to describe the size and dynamics of this bubble. A full solution would require solving the D7-brane equations of motion in a dynamic background, taking proper account of the boundary conditions at infinity. We can, however, make some progress within our Rindler approximation. Note first that, due to the scale invariance of Minkowski space, in our Rindler approximation the curvature scale of the initial static D7-brane at the tip ( $y = 0, z = z_0$ ) must be set by  $z_0$  [26]. Thus, for  $y \ll z_0$  we can model the initial configuration of the brane by the hyperplane  $z = z_0$ , with  $x_9 = 0$ . In terms of the light-cone Minkowski coordinates, the brane lies on the hyperbolic curve  $-UV = z_0^2$  with  $x_9 = 0$ .

At  $V = V_0$ , a point on the brane at impact parameter  $\rho$  will be shifted by an amount  $|\Delta U| = \mu\Phi(\rho)$ . Thus, immediately after the jump the profile of the branes is given by<sup>8</sup>

$$z(\rho) = \sqrt{z_0^2 - \frac{E}{2\pi T}\Phi(\rho)} = z_0\sqrt{1 - \frac{R_0}{\rho}}, \quad (4.9)$$

where

$$R_0 = \frac{2}{\pi} \frac{G_5 E}{T z_0^2} \quad (4.10)$$

and  $G_5 = G_{10}/(\pi^3 L^5)$ . We will comment further on the fact that  $R_0 \sim E$  in section 5.

Equation (4.9) describes a cylinder of radius  $R_0$  and height  $z_0$  which attaches smoothly to an infinite plane at  $z = z_0$ . Our approximation is valid for  $R_0 \ll z_0$ , in which case the cylinder is tall and narrow. It therefore has a tendency to contract. Furthermore, as shown in the appendix, over most of our Rindler region (for  $\rho < \rho_* = (R_0 z_0^2)^{1/3}/2$ , or  $z < z_*$  with  $z_* \approx z_0 - (R_0^2 z_0)^{1/3}$ ) the bubble nucleates with  $\partial\rho/\partial V < 0$ . Thus, unless other influences from beyond  $z_*$  can arrive in time to prevent it, this part of the tube will collapse.

We now show that no such influences can arrive in time to prevent collapse. Some care is required due to the fact that our initial data is given on the surface  $V = V_0, z = z(\rho)$ , which is not a constant time surface in any natural coordinate system. To begin, consider a slice of the brane at constant  $z$ . If no influences arrive to slow the collapse, this part of the brane will collapse at  $V = V_0 + \Delta V$  for

$$\Delta V = \rho \left( -\frac{\partial\rho}{\partial V} \right)_z^{-1} = \frac{V_0}{(\rho_*/\rho)^3 - 1}, \quad \rho < \rho_*, \quad (4.11)$$

---

<sup>8</sup>When the falling object is localized on the  $S^5$  one obtains instead

$$z(\rho) = \sqrt{z_0^2 - \frac{E}{2\pi T}\Phi(\rho)} = z_0\sqrt{1 - \left(\frac{R_{loc}}{\rho}\right)^6},$$

$$(R_{loc})^6 = \frac{4}{3\Omega_7} \frac{G_{10} E}{T z_0^2}.$$

where in the last step we have used results from the appendix. Recalling that  $U = -z^2/V$  we see that an event at which a point on the cylinder collapses to zero size has spacetime coordinates  $(V, U, \rho) \sim (V_0 + \Delta V, -z_0^2/V_0 + \Delta V z_0^2/V_0^2, 0)$ , where we have assumed  $\Delta V/V_0 \ll 1$ . On the other hand, the event at  $V = V_0$  where  $\partial\rho/\partial V$  becomes positive has spacetime coordinates  $(V_* = V_0, U_* = -z_*^2/V_*, \rho_*) \sim (V_0, -z_0^2/V_0, \rho_*)$ . The spacetime interval between these events is therefore

$$\Delta s^2 = -\Delta U \Delta V + (\Delta\rho)^2 \sim -\left(\frac{z_0}{(\rho_*/\rho)^3 - 1}\right)^2 + \rho_*^2, \quad (4.12)$$

which is positive for  $\rho < \bar{\rho} \sim \frac{1}{2^{4/3}} R_0^{4/9} z_0^{5/9}$ . Thus, the tube collapses at least out to height  $\bar{z} = z_0 \sqrt{1 - \frac{R_0}{\bar{\rho}}} \approx z_0 \left(1 - 2^{1/3} \left(\frac{R_0}{z_0}\right)^{5/9}\right)$ .

It is interesting to ask about the rate at which the bubble collapses. However, this question is complicated by several considerations associated with the fact that the bubble is far from even local thermodynamic equilibrium. First, the bubble does not form at a single value of the gauge theory time  $t$ . Instead, it forms on the null surface  $V = V_0$ . Second, there is some ambiguity as to what one wishes to call the “size” of the bubble. The naive bubble size is  $R_0$ , the radius of the cylinder of D7-brane intersecting the horizon at  $V = V_0$ . However, we have seen that the rather larger region of the brane out to  $\rho = \bar{\rho} \gg R_0$  eventually collapses. A causality calculation similar to the one above then shows that any excitation of the brane (e.g., a meson) which begins at  $\rho < \hat{\rho} \sim 2(R_0^2 z_0)^{1/3}$  is necessarily caught in the collapsing bubble, so that it is the scale  $\hat{\rho}$  which governs the region in which meson propagation is highly disrupted. In terms of the gravity side of the gauge/gravity correspondence, we will tentatively describe these effects as a bubble of proper size  $R_0$  surrounded by a rather larger region in which propagation of disturbances on the D7-brane is highly disrupted (though we again emphasize that in reality the entire region is far from any local thermodynamic equilibrium). Using the metric (4.1) to translate distances to the gauge theory, for small  $R_0/z_0$  we have a bubble of size  $\tilde{R}_0 = R_0/(\pi T L) \sim E/(\pi(0.15)^2 N_c^2 T^2)$ , surrounded by a large halo that interferes with meson propagation.

On the other hand, the time interval  $\Delta t$  between the creation and collapse of the bubble is a well-defined quantity. Using  $V = z e^{2\pi T t}$  and  $\Delta V/V_0 \ll 1$ , we find

$$\begin{aligned} \Delta t &\sim \frac{\Delta V}{2\pi T V_0} \\ &\sim \frac{\rho_*}{2\pi T z_0} = \frac{1}{4\pi T} \left(\frac{R_0}{z_0}\right)^{1/3} = \frac{1}{4(\pi T)^{2/3}} \left(\frac{\tilde{R}_0}{0.15}\right)^{1/3} \quad \text{for } \rho = \bar{\rho}. \end{aligned} \quad (4.13)$$

When the tube collapses, the motion can no longer be described using the classical equations of motion for the D7-brane. However, one expects that the collapsed tube breaks off from the rest of the D7-brane, perhaps annihilating in a shower of radiation. What remains is a D7-brane still somewhat distorted from its equilibrium configuration, which then oscillates in  $z$  until the remaining energy is dispersed.

Let us briefly comment on larger bubbles, beyond what can be accurately described in our Rindler approximation. Recall that  $z_0 \gtrsim 0.15L$  so that  $R_0 \gg z_0$  implies  $R_0 \gg L$ .

Thus, the dynamics of such bubbles will proceed slowly enough to be affected by the shape of the branes in the asymptotic region of the spacetime. It is just this asymptotic region which controls the difference in energy between the most stable black hole and Minkowski embeddings found in [24, 25]. Since we work at a temperature where the Minkowski embedding is thermodynamically stable, it is clear that the energetics of this region cause the bubble to contract; i.e., the bubble is compressed by thermodynamic pressure.

While our Rindler approximation does not allow us to calculate the precise timescale for this collapse, the collapse is given by the motion of a probe D7-brane in the black D3-brane background. As a result, the collapse timescale must be of the form  $T^{-1}$  times a function of  $R_0$ , the initial height  $z_0$ , and the AdS scale  $L$ . The multiplicative factor of  $T^{-1}$  comes from the metric (4.7) and appears when translating proper time to coordinate time. The proper time, however, cannot depend on the temperature  $T$  since, in the particular model considered, one may change  $T$  via a change of coordinates. In gauge theory terms, this is associated with the scale invariance of the  $N = 4$  super-Yang-Mills theory to which the quarks have been added as a small perturbation. From the gauge theory perspective the timescale is determined by  $T, T_f$ , and the bubble size  $\tilde{R}_0$  and is otherwise independent of  $\lambda, N_c, N_f$ . Because additional dependence on  $T$  appears when expressing  $z_0$  in terms of gauge theory parameters,  $\Delta t$  need not be proportional to  $T^{-1}$ .

It is also interesting to analyze the bubble dynamics directly in gauge theory terms. In contrast to the above, we now assume that the 't Hooft coupling  $\lambda$  is small in order that we may calculate reliably.

In the gauge theory, the bubble of melted mesons is distinguished from its surrounding plasma by the presence of deconfined quarks. The bubble shrinks due to processes where these quarks annihilate to form gluons which may then leave the surface of the bubble and carry away energy. Quarks can also combine to form mesons, but this process is suppressed by a factor of  $1/N_c$  in the large  $N_c$  limit. The quark-quark-gluon vertex factor is  $g_{YM} = \sqrt{\lambda/N_c}$  so the production rate scales as

$$N_f N_c^2 \left( \sqrt{\frac{\lambda}{N_c}} \right)^2 \sim \lambda N_f N_c, \quad (4.14)$$

in the limit of large  $N_c$ . Here the factor  $N_f N_c^2$  comes from summing over initial states. Since there are  $N_f$  species of heavy quarks, and since each species comes in  $N_c$  colors, the lifetime of the bubble scales as  $N_f^0 N_c^0$ . This result matches the scaling with  $N_c, N_f$  found on the gravity side at large  $\lambda$ , where collapse of the bubble was merely classical brane dynamics in a fixed background.

One may expect the bubble to decay only due to interactions near the surface so that the lifetime of the bubble scales with the volume-to-surface area ratio  $\tilde{R}_0$ . This expectation is justified when the interior of the bubble is in local thermal equilibrium so that it is equally likely there for two quarks to combine into a gluon, or a gluon to decay into two quarks. However, since it exists only for a time  $\Delta t \ll 1/T$ , our bubble is in fact quite far from thermal equilibrium and it is possible that the entire bubble contributes to the decay of the bubble.

## 5. Discussion

The above sections used gauge/gravity duality to describe two types of processes involving the rapid transfer of localized energy to deconfined plasmas at large  $\lambda, N_c$ . The first process involves high energy collisions with balls of deconfined plasma surrounded by a confining phase, while the second involves the localized heating of a deconfined plasma. Both processes correspond to collisions with black holes in the gravity dual, where they result in the nucleation of a new “arm” of the horizon that reaches out in the direction of the incident object. In the first case, the arm stretches into a gauge theory direction while in the second it extends in the holographic direction. We have described the shape of this arm in the limit where the incident object is highly boosted and where one considers only the region close to the original black hole. After the collision, the arm is absorbed into the body of the black hole, though we have not described this process in any detail.

Within the context of this duality, our results show that highly boosted particles incident on a plasma ball induce the formation of “virtual arms” which, though they contain no plasma themselves, will with large probability cause any additional particles passing through them to be captured by the plasma (see Fig. 7). These virtual arms summarize the interactions of both the original plasma ball and the incident highly boosted particle with any additional particles that may be present. The shape of a virtual arm was determined in section 3 (see equation (3.5)), where the arm length was found to scale with the energy of the incident particle and inversely with a power of the cut-off  $\tilde{r}$  on the transverse size.

It is straightforward to generalize our single-particle analysis to the case of a dense cluster of particles, such as might be present in a pulsed beam. There are two essential points: *i*) The arm shape is driven by the Aichelburg-Sexl potential which is determined by solving a Poisson equation whose source is the incident energy. Thus, this potential satisfies a superposition principle. *ii*) Since the dynamical timescale for the horizon is  $1/T$ , the response of the horizon is independent of the distribution of the incident energy along the direction of motion as long as the entire pulse of energy arrives in a time  $\Delta t \ll 1/T$ . Thus, (3.5) may be used to calculate the length of the virtual arm induced collectively by particles in the cluster by taking the energy  $E$  to include all incident particles that arrive within the relaxation timescale  $1/T$  and  $r$  to describe the size of the incoming cluster of particles. In fact, if the cluster is rotationally invariant about the direction of motion, (3.5) can be used to compute the arm shape by taking  $E(r)$  to be the energy contained within a cylinder of radius  $r$ .

The scaling with  $E$  is universal in the limit of a thin relativistic beam, independent of the detailed model for the duality. The scaling with the cut-off  $r$  depends only on the dimension of the gravity dual. It would therefore be interesting to compare both scalings with calculations in a weakly coupled gauge theory and with experiments that might one day be performed with QCD plasmas. Such experiments could provide a new test of the extent to which QCD plasmas might be described by a classical gravity dual, independent of the details of any particular model.

We also obtained results in the context of local heating of plasmas. Not surprisingly,

we found that such heating can produce bubbles of a higher temperature phase, but that these bubbles are unstable and collapse. In terms of the proper bubble size  $R_0$  in the bulk or the proper bubble size  $\tilde{R}_0$  in the gauge theory, we were able to study the dynamics in detail for  $T \sim T_f$ , large  $\lambda$ , and small bubbles  $R_0 \ll z_0$ ,  $\tilde{R}_0 \ll 1/T$ . There we found that the bubbles are surrounded by a much larger region where meson propagation is highly disrupted. We also found that the bubbles collapse within a time  $\Delta t \sim \frac{1}{4(\pi T)^{2/3}} \left(\frac{\tilde{R}_0}{0.15}\right)^{1/3}$ . More generally (for larger  $\tilde{R}_0$ , smaller  $T$ , or small  $\lambda$ ) the collapse time may depend on  $T, T_f$ , and  $\tilde{R}_0$ , but must remain otherwise independent of  $\lambda, N_f, N_c$ .

A result of particular interest is the dependence of the bubble radius on both the energy  $E$  and the temperature  $T$ . Recall that we considered an example four-dimensional gauge theory with  $N_f$  flavors of fundamental matter in which the mesons were stable at  $T < T_f$ , but where the bubble corresponded to a phase in which mesons are melted. It is clear that little of the incident energy is transferred to the mesons, so the main effect is a local heating of the plasma. Since the specific heat of the system is of order  $N_c^2$  and the mesons melt at temperature  $T_f$ , one might therefore expect the bubble size to be of order

$$\tilde{R}_{naive} \sim \left( \frac{E}{(T_f - T) T_f^3 N_c^2} \right)^{1/3} \quad (5.1)$$

as there is only enough energy to raise the temperature from  $T$  to  $T_f$  over a region of this size.

However, at least when  $T \sim T_f$ , the bubbles that form in our processes are in fact of size  $\tilde{R}_0 \sim \frac{E}{\pi(0.15)^2 T_f^2 N_c^2}$ , where we have translated (4.10) to gauge theory parameters using  $\tilde{R}_0 = R_0/(\pi T L)$ ,  $z_0 \sim L$  and (4.3). Thus, the bubble size is independent of  $T - T_f$  and, in the limit of large  $E$ , the actual bubble size  $\tilde{R}_0$  is much *larger* than  $\tilde{R}_{naive}$ . This is due to the fact that the bubble is quite far from thermal equilibrium. In fact, from the bulk perspective the black hole arm that pulls the probe brane behind the horizon exists only for the time scale  $\Delta t \sim 1/T$  typical of thermal fluctuations. Thus, there is no reason to assign the arm an energy density characteristic of thermal equilibrium at temperature  $T_f$ .

Our analysis considered only physics associated with the region close to the original black hole horizon and cases where the incident particles approach the black hole at relativistic speeds. In such regimes, the behavior of the black hole horizon is universal and independent of the details of any particular duality. One may therefore hope that this limit describes universal physics of deconfined plasmas at large  $N_c$ . However, it is also clear that there is much to learn from the details of particular models in regimes where these limits do not apply. Some such extensions of this work may be straightforward, such as taking into account the details of the black D3-brane solution and the various D7-brane embeddings found in [24, 25]. Other more complicated extensions might involve studying the collisions of two plasma balls. Such situations are also more complicated from the bulk viewpoint and may require sophisticated numerical simulations. However, recent progress (see e.g., [28]) in simulating black hole collisions in 3+1 dimensions suggests that such calculations may nevertheless prove tractable in the near future.

## Acknowledgements

We thank David Mateos for his patient explanations of AdS/QCD with flavor and for many enlightening discussions. AV would also like to thank Anshuman Maharana and Matthew Roberts for several useful discussions. This work was supported in part by the National Science Foundation under Grant No. PHY05-55669, and by funds from the University of California.

## A. Brane dynamics in the Aichelburg-Sexl solution

In this appendix we provide a brief calculation of the D7-brane's initial velocity induced by crossing the Aichelburg-Sexl shock wave. We find that there is a region between  $z = 0$  and  $z \sim z_0 - (R_0^2 z_0)^{1/3}$  where the bubble nucleates in a contracting phase, as claimed in section 4.2

In analogy to the solutions for null geodesics found in section 2.1, let us assume that the D7-brane configuration is described by specifying  $U(V, \rho)$ . Hence, the induced metric on the brane takes the form

$$ds_{brane}^2 = \left( -\frac{\partial U}{\partial V} + \mu\Phi(\rho)\delta(V - V_0) \right) dV^2 + \frac{\partial U}{\partial \rho} d\rho dV + d\rho^2 + \rho^2 d\Omega_2^2 + dy^2 + y^2 d\Omega_3^2. \quad (\text{A.1})$$

As a result, the Lagrangian density appearing in the DBI action for the brane is

$$\mathcal{L} \propto \rho^2 \sqrt{\frac{\partial U}{\partial V} + \frac{1}{4} \left( \frac{\partial U}{\partial \rho} \right)^2 - \mu\Phi(\rho)\delta(V - V_0)}. \quad (\text{A.2})$$

Based on the discussion in section 4.2, we choose an ansatz for  $U(V, \rho)$  of the form

$$U(V, \rho) = -\frac{z_0^2}{V} + h(V, \rho)\Theta(V - V_0), \quad (\text{A.3})$$

where  $h(V, \rho)$  is continuous in  $V$  and satisfies  $h(V_0, \rho) = |\Delta U| = \mu\Phi(\rho)$ . Using this ansatz and the equation of motion obtained from (A.2), we find that immediately after the shock wave passes

$$\frac{\partial U}{\partial V} = \frac{z_0^2}{V_0^2} + \frac{\partial h}{\partial V} \Big|_{V=V_0} = \frac{z_0^2}{V_0^2} - \frac{\mu^2 \Phi'(\rho)^2}{8}. \quad (\text{A.4})$$

Now, recall that the Rindler coordinate  $z$  is related to  $U, V$  through  $z = \sqrt{-UV}$ , so the velocity in the  $z$  direction (at fixed  $\rho$ ) is

$$\left( \frac{\partial z}{\partial V} \right)_\rho = -\frac{1}{2\sqrt{-UV}} \left( U + V \left( \frac{\partial U}{\partial V} \right)_\rho \right). \quad (\text{A.5})$$

The radial velocity of the cylinder (at fixed  $z$ ) is then given by

$$\left( \frac{\partial \rho}{\partial V} \right)_z = -\left( \frac{\partial z}{\partial V} \right)_\rho \left( \frac{\partial z}{\partial \rho} \right)_V^{-1} = \frac{1}{V_0} \left( \rho - \frac{R_0 z_0^2}{8\rho^2} \right), \quad (\text{A.6})$$

where we have used  $z(V_0, \rho) = z_0 \sqrt{1 - R_0/\rho}$  and  $R_0$  is defined in (4.10). Equation (A.6) implies that  $\partial\rho/\partial V$  is indeed negative for  $\rho < \rho_* \equiv \frac{(R_0 z_0^2)^{1/3}}{2}$ , though it is positive for  $\rho > \rho_*$ .

## References

- [1] J. M. Maldacena, “The large N limit of superconformal field theories and supergravity,” *Adv. Theor. Math. Phys.* **2** (1998) 231 [*Int. J. Theor. Phys.* **38** (1999) 1113] [arXiv:hep-th/9711200].
- [2] O. Aharony, S. S. Gubser, J. M. Maldacena, H. Ooguri, and Y. Oz, “Large N field theories, string theory and gravity,” *Phys. Rept.* **323** (2000) 183 [arXiv:hep-th/9905111].
- [3] E. Witten, “Anti-de Sitter space, thermal phase transition, and confinement in gauge theories,” *Adv. Theor. Math. Phys.* **2** (1998) 505 [arXiv: hep-th/9803131].
- [4] G. Policastro, D. T. Son, and A. O. Starinets, “The shear viscosity of strongly coupled N = 4 supersymmetric Yang-Mills plasma,” *Phys. Rev. Lett.* **87**, 081601 (2001) [arXiv:hep-th/0104066].  
G. Policastro, D. T. Son, and A. O. Starinets, “From AdS/CFT correspondence to hydrodynamics,” *JHEP* **0209**, 043 (2002) [arXiv:hep-th/0205052].  
G. Policastro, D. T. Son, and A. O. Starinets, “From AdS/CFT correspondence to hydrodynamics II: Sound waves,” *JHEP* **0212**, 054 (2002) [arXiv:hep-th/0210220].  
C. P. Herzog, “The hydrodynamics of M-theory,” *JHEP* **0212**, 026 (2002) [arXiv:hep-th/0210126].  
C. P. Herzog, “The sound of M-theory,” *Phys. Rev. D* **68** (2003) 024013 [arXiv:hep-th/0302086].  
A. Buchel and J. T. Liu, “Universality of the shear viscosity in supergravity,” *Phys. Rev. Lett.* **93**, 090602 (2004) [arXiv:hep-th/0311175].  
P. Kovtun, D. T. Son, and A. O. Starinets, “Holography and hydrodynamics: Diffusion on stretched horizons,” *JHEP* **0310**, 064 (2003) [arXiv:hep-th/0309213].  
P. Kovtun, D. T. Son, and A. O. Starinets, “Viscosity in strongly interacting quantum field theories from black hole physics,” *Phys. Rev. Lett.* **94**, 111601 (2005) [arXiv:hep-th/0405231].  
A. Buchel, “On universality of stress-energy tensor correlation functions in supergravity,” *Phys. Lett. B* **609**, 392 (2005) [arXiv:hep-th/0408095].  
P. Benincasa, A. Buchel, and A. O. Starinets, “Sound waves in strongly coupled non-conformal gauge theory plasma,” *Nucl. Phys. B* **733**, 160 (2006) [arXiv:hep-th/0507026].  
For further references see [8].
- [5] A. Parnachev and A. Starinets, “The silence of the little strings,” *JHEP* **0510**, 027 (2005) [arXiv:hep-th/0506144].  
P. Benincasa, A. Buchel, and A. O. Starinets, “Sound waves in strongly coupled non-conformal gauge theory plasma,” *Nucl. Phys. B* **733**, 160 (2006) [arXiv:hep-th/0507026].  
J. Mas and J. Tarrío, “Hydrodynamics from the Dp-brane,” *JHEP* **0705**, 036 (2007) [arXiv:hep-th/0703093].  
A. Buchel, “Bulk viscosity of gauge theory plasma at strong coupling,” arXiv:0708.3459 [hep-th] and references therein.
- [6] H. Liu, K. Rajagopal, and U. A. Wiedemann, “Calculating the jet quenching parameter from AdS/CFT,” *Phys. Rev. Lett.* **97**, 182301 (2006) [arXiv:hep-ph/0605178].  
C. P. Herzog, A. Karch, P. Kovtun, C. Kozcaz, and L. G. Yaffe, “Energy loss of a heavy quark moving through N = 4 supersymmetric Yang-Mills plasma,” *JHEP* **0607**, 013 (2006) [arXiv:hep-th/0605158].  
J. Casalderrey-Solana and D. Teaney, “Heavy quark diffusion in strongly coupled N = 4 Yang-Mills,” *Phys. Rev. D* **74** 085012 (2006) [arXiv:hep-ph/0605199].

- S. S. Gubser, “Drag force in AdS/CFT,” *Phys. Rev. D* **74** 126005 (2006) [arXiv:hep-th/0605182].  
 For a review see: H. Liu, “Heavy ion collisions and AdS/CFT,” *J. Phys. G* **34**, S361 (2007) [arXiv:hep-ph/0702210].
- [7] See for example:  
 H. Nastase, “The RHIC fireball as a dual black hole,” [arXiv:hep-th/0501068].  
 E. Shuryak, S. J. Sin, and I. Zahed, “A gravity dual of RHIC collisions,” *J. Korean Phys. Soc.* **50**, 384 (2007) [arXiv:hep-th/0511199].  
 R. A. Janik and R. Peschanski, “Asymptotic perfect fluid dynamics as a consequence of AdS/CFT,” *Phys. Rev. D* **73**, 045013 (2006) [arXiv:hep-th/0512162].  
 H. Nastase, “More on the RHIC fireball and dual black holes,” [arXiv:hep-th/0603176].  
 R. A. Janik and R. Peschanski, “Gauge / gravity duality and thermalization of a boost-invariant perfect fluid,” *Phys. Rev. D* **74**, 046007 (2006) [arXiv:hep-th/0606149].  
 R. A. Janik, “Viscous plasma evolution from gravity using AdS/CFT,” *Phys. Rev. Lett.* **98**, 022302 (2007) [arXiv:hep-th/0610144].  
 S. Lin and E. Shuryak, “Toward the AdS/CFT gravity dual for high energy heavy ion collisions,” [arXiv:hep-ph/0610168].  
 J. J. Friess, S. S. Gubser, G. Michalogiorgakis, and S. S. Pufu, “Expanding plasmas and quasinormal modes of anti-de Sitter black holes,” *JHEP* **0704**, 080 (2007) [arXiv:hep-th/0611005].  
 E. Shuryak, “Emerging theory of strongly coupled quark-gluon plasma,” [arXiv:hep-ph/0703208].  
 M. P. Heller and R. A. Janik, “Viscous hydrodynamics relaxation time from AdS/CFT,” *Phys. Rev. D* **76**, 025027 (2007) [arXiv:hep-th/0703243].
- [8] D. Mateos, “String Theory and Quantum Chromodynamics,” arXiv:0709.1523 [hep-th].
- [9] S. S. Gubser, I. R. Klebanov, and A. W. Peet, “Entropy and Temperature of Black 3-Branes,” *Phys. Rev. D* **54**, 3915 (1996) [arXiv:hep-th/9602135].  
 S. S. Gubser, I. R. Klebanov, and A. A. Tseytlin, “Coupling constant dependence in the thermodynamics of  $N = 4$  supersymmetric Yang-Mills theory,” *Nucl. Phys. B* **534**, 202 (1998) [arXiv:hep-th/9805156].
- [10] D. Teaney, “Effect of shear viscosity on spectra, elliptic flow, and Hanbury Brown-Twiss radii,” *Phys. Rev. C* **68** 034913 (2003) [arXiv:nucl-th/0301099].  
 E. Shuryak, “Why does the quark gluon plasma at RHIC behave as a nearly ideal fluid?,” *Prog. Part. Nucl. Phys.* **53**, 273 (2004) [arXiv:hep-ph/0312227].
- [11] “Black Holes: The Membrane Paradigm,” R. Price, K. Thorne, D.A. MacDonald, eds. (Yale University Press, 1986).
- [12] U. Sperhake et al, in preparation.
- [13] S. L. Shapiro and S. A. Teukolsky, “Collisions of relativistic clusters and the formation of black holes,” *Phys. Rev. D* **45**, 2739 (1992).  
 P. Anninos, D. Hobill, E. Seidel, L. Smarr, and W. M. Suen, “The collision of two black holes,” *Phys. Rev. Lett.* **71**, 2851 (1993) [arXiv:gr-qc/9309016].  
 S. A. Hughes, C. R. Keeton, P. Walker, K. T. Walsh, S. L. Shapiro, and S. A. Teukolsky, “Finding black holes in numerical space-times,” *Phys. Rev. D* **49**, 4004 (1994).  
 A. M. Abrahams, G. B. Cook, S. L. Shapiro, and S. A. Teukolsky, “Solving Einstein’s equations for rotating space-times: Evolution of relativistic star clusters,” *Phys. Rev. D* **49**, 5153 (1994).



- P. Anninos *et al.*, “Dynamics Of Apparent And Event Horizons,” *Phys. Rev. Lett.* **74**, 630 (1995) [arXiv:gr-qc/9403011].
- J. Libson, J. Masso, E. Seidel, W. M. Suen, and P. Walker, “Event horizons in numerical relativity. 1: Methods and tests,” *Phys. Rev. D* **53**, 4335 (1996) [arXiv:gr-qc/9412068].
- R. A. Matzner, H. E. Seidel, S. L. Shapiro, L. Smarr, W. M. Suen, S. A. Teukolsky, and J. Winicour, “Geometry of a black hole collision,” *Science* **270**, 941 (1995).
- S. L. Shapiro, S. A. Teukolsky, and J. Winicour, “Toroidal Black Holes And Topological Censorship,” *Phys. Rev. D* **52**, 6982 (1995).
- [14] S. W. Hawking and G. F. R. Ellis, “The large scale structure of space-time,” Cambridge University Press (1973).
- [15] R. M. Wald, “General Relativity,” University of Chicago Press (1984).
- [16] A. J. Amsel, D. Marolf, and A. Virmani, “The Physical Process First Law for Bifurcate Killing Horizons,” arXiv:0708.2738 [gr-qc].
- [17] P. C. Aichelburg and R. U. Sexl, “On the Gravitational Field of a Massless Particle,” *Gen. Rel. Grav.*, **2**, 303-312 (1971).
- [18] V. Ferrari, P. Pendenza, and G. Veneziano, “Beam-Like Gravitational Waves and Their Geodesics,” *Gen. Rel. Grav.*, **20**, 1185-1191 (1988).
- [19] T. Dray and G. ’t Hooft, “The Gravitational Shock Wave of a Massless Particle,” *Nucl. Phys. B*, **253**, 173-188 (1985).
- [20] O. Aharony, S. Minwalla, and T. Wiseman, “Plasma-balls in large N gauge theories and localized black holes,” *Class. Quant. Grav.* **23**, 2171 (2006) [arXiv:hep-th/0507219].
- [21] G. T. Horowitz and R. C. Myers, “The AdS/CFT correspondence and a new positive energy conjecture for general relativity,” *Phys. Rev. D* **59**, 026005 (1999) [arXiv:hep-th/9808079].
- [22] A. Karch and L. Randall, “Open and closed string interpretation of SUSY CFT’s on branes with boundaries,” *JHEP* **0106** (2001) 063 [arXiv: hep-th/0105132].
- [23] A. Karch and E. Katz, “Adding flavor to AdS/CFT,” *JHEP* **0206** (2002) 043 [arXiv: hep-th/0205236].
- [24] D. Mateos, R. C. Myers, and R. M. Thomson, “Holographic phase transitions with fundamental matter,” *Phys. Rev. Lett.* **97** (2006) 091601 [arXiv: hep-th/0605046].
- [25] D. Mateos, R. C. Myers, and R. M. Thomson, “Thermodynamics of the brane,” *JHEP* **0705**, 067 (2007) [arXiv: hep-th/0701132].
- [26] V. P. Frolov, “Merger transitions in brane-black-hole systems: Criticality, scaling, and self-similarity,” *Phys. Rev. D* **74** (2006) [arXiv: gr-qc/0604114].
- [27] R. Gregory and R. Laflamme, “Black strings and p-branes are unstable,” *Phys. Rev. Lett.* **70**, 2837 (1993) [arXiv:hep-th/9301052].
- [28] F. Pretorius, “Binary Black Hole Coalescence,” arXiv:0710.1338 [gr-qc].